

# The research on the natural ventilation cooling for photovoltaic solar cell

KUN-RU MA<sup>1</sup>, YI-JUN WANG<sup>2</sup>, NA-NA HOU<sup>3</sup>,  
RUI-JIAO YU<sup>4</sup>, XIAO-DONG XIAN<sup>5</sup>

**Abstract.** This paper mainly research the thermal properties and the battery temperature of the heat transfer process in different natural ventilation cooling for photovoltaic solar cell. Establishing the physical model and mathematical model of the photovoltaic solar cell in different natural ventilation cooling. Then it summarizes the changes about temperature distribution and heating of the photovoltaic solar cell in different natural ventilation cooling with different factors: outdoor temperature, wind speed, and solar radiation, etc. The conclusion of this paper can provide theoretical basis for different natural ventilation cooling systems of the photovoltaic solar cell in terms of design, construction and operating maintenance.

**Key words.** Photovoltaic solar cell, natural ventilation cooling, battery temperature, thermal dissipation.

## 1. Introduction

The rapid development of human society and the world economy can not do without the energy exploitation and utilization, therefore the exploitation of clean energy has not only become the most important strategic task of national energy sustainable development, but also a basic trend of modern energy utilization [1,4]. For instance, Solar energy has been widely applied in clean energy field with the advantage of clean, safe, renewable and wide distribution. Natural ventilation cooling technology has superiority on no noise, no pollution, low failure rate and easy maintenance. And its applied technique has been mature gradually and safe as well as reliable [5,6]. At present, there is rare study on new system of natural ventilation cooling of photovoltaic panel. The new system uses different natural ventilation cooling method

---

<sup>1</sup>Workshop 1 - Department of Civil, the Civil Engineering College, Hebei University of Science and Technology, Shijiazhuang, China; e-mail: [makunru@163.com](mailto:makunru@163.com)

<sup>2</sup>Workshop 2 - Department of Civil, Hebei University of Water Resources and Electric Engineering, Cangzhou, China; e-mail: [sufeng1018@163.com](mailto:sufeng1018@163.com)

<sup>3</sup>Workshop 3 - Department of Civil, the Civil Engineering College, Hebei University of Science and Technology, Shijiazhuang, China; e-mail: [1585886625qq.com](mailto:1585886625qq.com)

such as natural ventilation without cooling measures, adding fins on the PV back and adding fins and the air duct on the PV back to influence heat radiation of photovoltaic solar panels, and then reduce battery plate temperature. The schematic of the different natural ventilation cooling systems for PV panels is shown in figure 1-3.

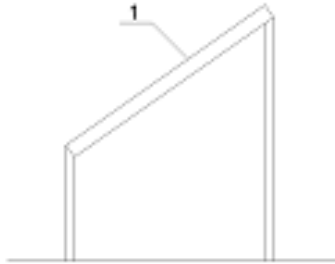


Fig. 1. Schematic figure of natural ventilation photovoltaic solar system without cooling back 1- Photovoltaic solar panels

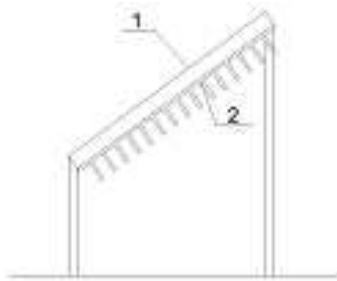


Fig. 2. Schematic figure of photovoltaic solar system with fins on the PV back 1-2- Fins 3-Plastic board

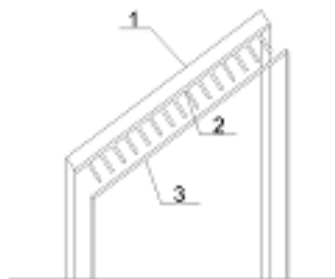


Fig. 3. Schematic figure of photovoltaic solar system with fins and air duct on PV back

## 2. Establishment of the model

### 2.1. The physical mode

When the natural ventilation of solar panels is considered, due to the influence of meteorological factors, the flow direction and velocity of up and down surface air about solar panels may change at any time. If only the solar panels and its adjacent space are treated as simulation area, then the import and export of the boundary conditions about CFD simulation is difficult to given accurately. Therefore, it is necessary to take the up and down surface of solar panels and its surrounding space together as the computational domain of CFD simulation.

Three physical models are established in this paper. In the first mode, the space size is 10m×10m and two solar panels which include experiment and comparison were installed. Then the size of installing solar panels is 1650mm×990mm×35mm (L×W×H), and the angle with the ground is 35 degrees. At last, start and stop position of X axis projection is 4.5m - 5.3m. On the basis of model one, solar panel back of the second model has fins which use aluminum. The spacing between the top and bottom of the fins is 67.5mm, and the distance between the left and right of the fins is 57mm. The size of each fin is 240×120×120 (length×width×height). The fins increase the area of heat dissipation. The third model adds air duct which uses PP plastic plate with combination of solar chimney theory on the basis of second model. And the spacing of air duct is 30mm, 60mm and 90mm. The third model increases wind speed of the solar panels back and reduces the battery plate temperature. The physical parameters of materials about heat transfer for photovoltaic solar panel are shown in table 1. Table 1 physical parameters of different materials about heat transfer for photovoltaic solar panel

Name	Material	Physical parameter value		
		Density (kg/m <sup>3</sup> )	Specific heat capacity (KJ/(kg×k))	Thermal conductiv- ity (W/(m×k))
Photovoltaic solar panel	Glass	2500	750	1.4
Fin	Aluminum	2719	871	202.4
Air duct	PP plastic plate	920	2.1	0.21

### 2.2. Mathematical model

In this paper, CFD technology is applied to the photovoltaic panel which is in outdoor space. The differential equations about mass, momentum and energy conservation of the outdoor incompressible ideal gas is discrete and analytic solution is obtained. The paper uses two dimensional and turbulent flow model, and the battery plate is treated as plane heat source. Because of the influence of radiation factors, the type of model is Low - Re - K - $\varepsilon$ , which is double equation turbulence

model. And the finite volume method is used to disperse the governing equations. Finally, the solver for calculation is FLUENT solver. The mathematical model which is used in this paper is:

(1) Mass conservation equation

Every kind of flow problem should obey the law about conservation of mass. A mathematical description of the mass conservation equation can be expressed as[5]:

$$\frac{\partial \rho}{\partial t} + \frac{\partial(\rho u)}{\partial x} + \frac{\partial(\rho v)}{\partial y} + \frac{\partial(\rho w)}{\partial z} = 0(1-1)$$

The fluid in this paper is steady state flow, so the density does not change with time. Thus, change(1-1) into:

$$\frac{\partial(\rho u)}{\partial x} + \frac{\partial(\rho v)}{\partial y} + \frac{\partial(\rho w)}{\partial z} = 0(1-2)$$

Where,  $\rho$  is density;  $t$  is time;  $u, v$  and  $w$  are components of velocity vectors in the  $X, Y$ , and  $Z$  directions.

(2) Momentum conservation equation

Another fundamental law should be followed is conservation of momentum in any flow system. The fluid of model is an incompressible fluid. So the equations about conservation of momentum in three directions of  $x, y$  and  $z$  are derived[8,10]:

$$\begin{aligned} & \frac{\partial(\rho u)}{\partial t} + \frac{\partial(\rho u u)}{\partial x} + \frac{\partial(\rho u v)}{\partial y} + \frac{\partial(\rho u w)}{\partial z} \\ &= \frac{\partial}{\partial x} \left( \mu \frac{\partial u}{\partial x} \right) + \frac{\partial}{\partial y} \left( \mu \frac{\partial u}{\partial y} \right) + \frac{\partial}{\partial z} \left( \mu \frac{\partial u}{\partial z} \right) - \frac{\partial p}{\partial x} + F_x \end{aligned} \quad (1-3)$$

$$\begin{aligned} & \frac{\partial(\rho v)}{\partial t} + \frac{\partial(\rho v u)}{\partial x} + \frac{\partial(\rho v v)}{\partial y} + \frac{\partial(\rho v w)}{\partial z} \\ &= \frac{\partial}{\partial x} \left( \mu \frac{\partial v}{\partial x} \right) + \frac{\partial}{\partial y} \left( \mu \frac{\partial v}{\partial y} \right) + \frac{\partial}{\partial z} \left( \mu \frac{\partial v}{\partial z} \right) - \frac{\partial p}{\partial y} + F_y \end{aligned} \quad (1-4)$$

$$\begin{aligned} & \frac{\partial(\rho w)}{\partial t} + \frac{\partial(\rho w u)}{\partial x} + \frac{\partial(\rho w v)}{\partial y} + \frac{\partial(\rho w w)}{\partial z} \\ &= \frac{\partial}{\partial x} \left( \mu \frac{\partial w}{\partial x} \right) + \frac{\partial}{\partial y} \left( \mu \frac{\partial w}{\partial y} \right) + \frac{\partial}{\partial z} \left( \mu \frac{\partial w}{\partial z} \right) - \frac{\partial p}{\partial z} + F_z \end{aligned} \quad (1-5)$$

Where,  $p$  is pressure on a fluid element;  $\mu$  is dynamic viscosity;  $F_x, F_y$  and  $F_z$  are physical power of element in  $X, Y$  and  $Z$  direction, if only the physical gravity is considered, and the  $Z$  axis rises vertically, then  $F_x=0, F_y=0, F_z=-\rho g$ .

(3) Energy conservation equation

The fluid flow system with heat exchange should follow the fundamental law which is conservation of energy. Then the mathematical expression of energy conservation can be expressed as [11]:

$$\begin{aligned} & \frac{\partial(\rho T)}{\partial t} + \frac{\partial(\rho u T)}{\partial x} + \frac{\partial(\rho v T)}{\partial y} + \frac{\partial(\rho w T)}{\partial z} \\ &= \frac{\partial}{\partial x} \left( \frac{k}{c_p} \frac{\partial T}{\partial x} \right) + \frac{\partial}{\partial y} \left( \frac{k}{c_p} \frac{\partial T}{\partial y} \right) + \frac{\partial}{\partial z} \left( \frac{k}{c_p} \frac{\partial T}{\partial z} \right) + S_T \end{aligned} \quad (1-6)$$

Where,  $C_p$  is specific heat capacity;  $T$  is temperature;  $k$  is heat transfer coefficient of fluid;  $S_T$  are heat source of fluid and a part of thermal power which is changed by

mechanical energy of fluid under viscous action. The expression of  $S_T$  is shown in document [11].

(4)k -  $\varepsilon$  model for low reynolds number

The transport equation of k - $\varepsilon$  model for low reynolds number is expressed as[11,14]:

$$\frac{\partial(\rho k)}{\partial t} + \frac{\partial(\rho k u_i)}{\partial x_i} = \frac{\partial}{\partial x_j} \left[ \left( \mu + \frac{\mu_t}{\sigma_k} \right) \frac{\partial k}{\partial x_j} \right] + G_k - \rho \varepsilon - \left| 2\mu \left( \frac{\partial k^{1/2}}{\partial n} \right)^2 \right| \quad (1-7)$$

$$\begin{aligned} & \frac{\partial(\rho \varepsilon)}{\partial t} + \frac{\partial(\rho \varepsilon u_i)}{\partial x_i} \\ &= \frac{\partial}{\partial x_j} \left[ \left( \mu + \frac{\mu_t}{\sigma_\varepsilon} \right) \frac{\partial \varepsilon}{\partial x_j} \right] + \frac{C_{1\varepsilon} \varepsilon}{k} G_k |f_1| - C_{2\varepsilon} \rho \frac{\varepsilon^2}{k} |f_2| + \left| 2 \frac{\mu \mu_t}{\rho} \left( \frac{\partial^2 u}{\partial n^2} \right)^2 \right| \quad (1-8) \end{aligned}$$

$$\mu_t = C_\mu |f_\mu| \rho \frac{k^2}{\varepsilon} \quad (1-9)$$

Where,  $n$  is normal coordinate of the wall, in the actual calculation, the direction  $n$  takes one of the most satisfying conditions among the three  $x$ ,  $y$  and  $z$  approximately;  $u$  is the flow velocity in parallel with the wall, in the actual calculations,  $u$  is also treated similarly with  $n$ ;  $C_{1\varepsilon}, C_{2\varepsilon}, C_\mu, \sigma_k$  and  $\sigma_\varepsilon$  are constant, and  $C_{1\varepsilon} = 1.44, C_{2\varepsilon} = 1.92, C_\mu = 0.09, \sigma_k = 1.0, \sigma_\varepsilon = 1.3$ .

The mathematical expressions of the coefficients about  $f_1, f_2$  and  $f_\mu$  are as follows:

$$f_1 \approx 1.0(1 - 10)$$

$$f_2 \approx 1.0 - 0.3 \exp(-Re_t^2) \quad (1 - 11)$$

$$f_\mu = \exp(-2.5 / (1 + Re_t/50)) \quad (1 - 12)$$

$$Re_t = \rho k^2 / (\eta \varepsilon) \quad (1 - 13)$$

When  $Re_t$  is very large, both  $f_1, f_2$  and  $f_\mu$  are close to the 1. And  $Re_t$  is turbulent reynolds number.

(5)Radiation model

In this paper, the Rossland radiation model is used:

$$\frac{dI(\vec{r}, \vec{s})}{ds} + (a + \sigma_s) I(\vec{r}, \vec{s}) = an^2 \frac{\sigma T^4}{\pi} + \frac{\sigma_s}{4\pi} \int_0^{4\pi} I(\vec{r}, \vec{s}') \varphi(\vec{s}, \vec{s}') d\Omega' \quad (1-14)$$

Where  $r$  is position vector;  $s$  is direction vector;  $s'$  is scatter direction vector;  $s$  is length of path;  $a$  is absorption coefficient;  $n$  is index of refraction;  $\sigma_s$  is refraction coefficient;  $\sigma$  is Sigma Stephen Boltzmann constant;  $I$  is radiation intensity which depends on position and direction;  $T$  is local temperature;  $\phi$  is condensed phase of scattering phase function;  $\Omega'$  is solid angle;  $(a + \sigma_s)$  is extinction coefficient of medium.

Fig. 4 is a schematic diagram of the process about radiation heat transfer, and the outgoing radiation intensity is the result of incident radiation intensity through absorption, scattering, and emission of the gas medium / fluid medium along the way.

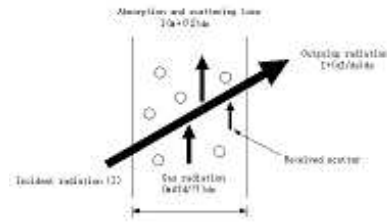


Fig. 4. Radiation heat transfer

### 3. The numerical simulation and results discussion

The finite volume method is used to discretize the computational domain and generate the mesh in this paper, and then the governing equations are discretized on the mesh. In addition, the Fluent software is used to simulate, and calculate the heat transfer equation to obtain the result by using algorithm of SIMLPE. In this paper, the changes of the temperature distribution and heat dissipation about photovoltaic solar cell in different natural ventilation cooling are obtained, and the system is in different factors: outdoor temperature, wind speed and solar radiation, etc.

*3.0.1. The changes about solar panel surface temperature distribution and heat radiation when the solar panel has fins or without fins* The distribution of temperature field and velocity field around the solar panel can be directly visualized by the temperature nephogram and velocity nephogram which are produced by FLUENT software. The temperature and velocity distribution around the photovoltaic panel is shown in figure 5 to figure 8.

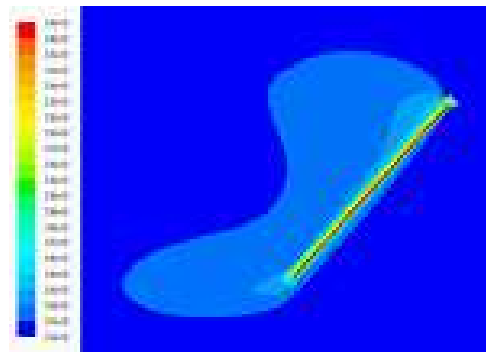


Fig. 5. The temperature distribution around the solar panel without fins

It can be seen through the temperature and velocity distribution around the photovoltaic solar panels: The temperature of solar panels is the highest, and temperature gradient above solar panels is the maximum. In addition, the distribution of temperature field is irregular, and the heat is mainly transferred to the above solar panel. The wind speed below the solar panel is greater than the above wind

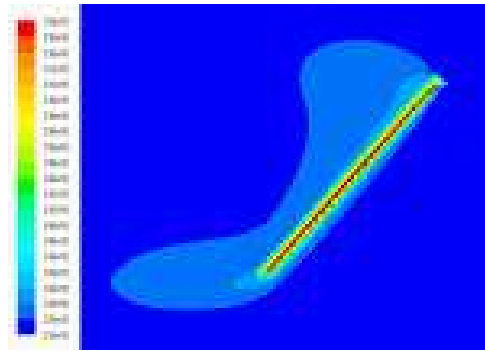


Fig. 6. The temperature distribution around the solar panel with fins

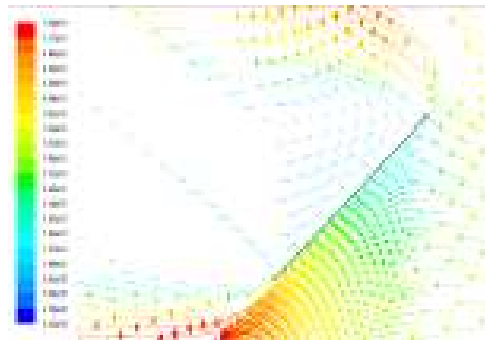


Fig. 7. The velocity distribution around the solar panel without fins

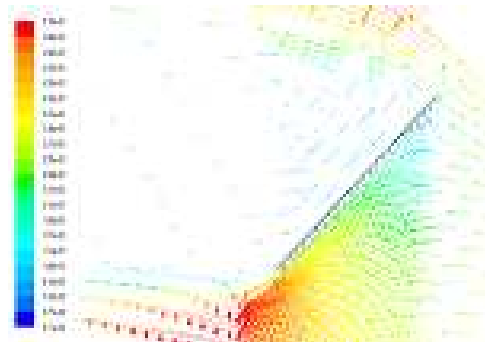


Fig. 8. The velocity distribution around the solar panel with fins

speed. In addition, because of the high temperature of the plate surface and the low temperature of surrounding, the circulation is formed between the upper plate and the fins.

Through the line chart of the numerical simulation data produced by the FLU-ENT software, we can observe the change of the solar panel surface temperature when the solar panel has fins or not. The surface temperature distribution of solar panel is shown in figure 9 to figure 10.

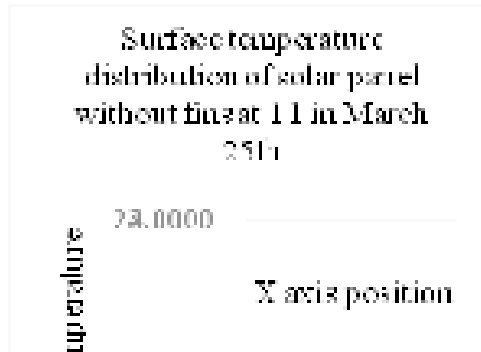


Fig. 9. surface temperature distribution of solar panels without fins

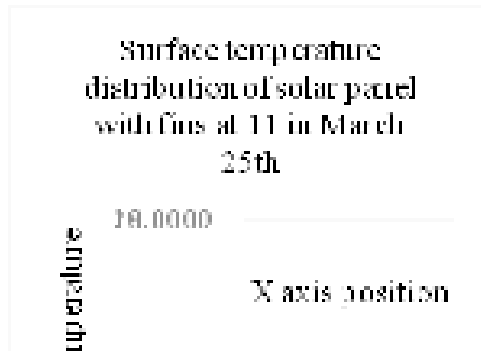


Fig. 10. surface temperature distribution of solar panels with fins

It can be seen through the temperature chart of photovoltaic solar cell: The temperature of solar panel which has fins is lower than solar panel without fins, the different value is three degree centigrade. So the heat dissipation of solar panel with fins is better than that without fins.

### ***3.1. Changes of solar panel surface temperature distribution and heat dissipation when solar panel has fins and different spacing duct and without fins***

In the temperature nephogram and velocity nephogram given by FLUENT software, we have a clearer understanding of the temperature field and velocity field distribution around the solar panel. The temperature and velocity distribution around the solar panel is shown in figure 11 to figure 18.

It can be seen from the photovoltaic solar panels temperature distribution diagram: the temperature distribution is not uniform, and the temperature of solar panels without fins is highest and uniform. In addition, the temperature gradient above the solar panel is the largest. And the heat mainly transferred to the above of solar panels.

The upper temperature of solar panel with fins and 30mm air duct is higher than



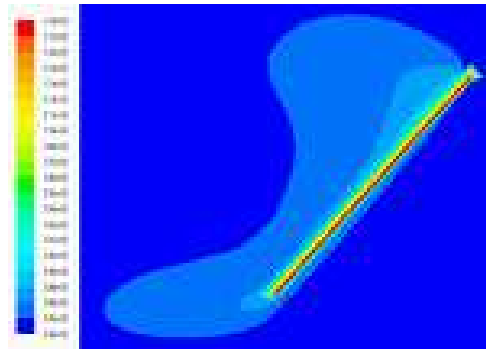


Fig. 11. temperature distribution diagram around the solar panel without fins

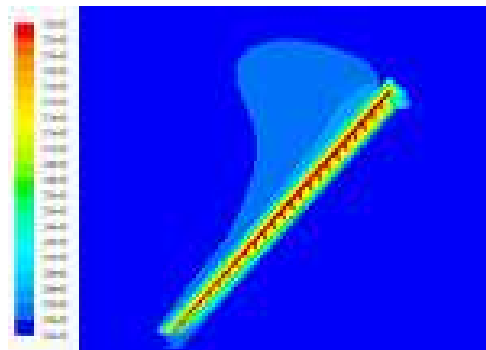


Fig. 12. temperature distribution diagram of solar panel with fins and 30mm air duct

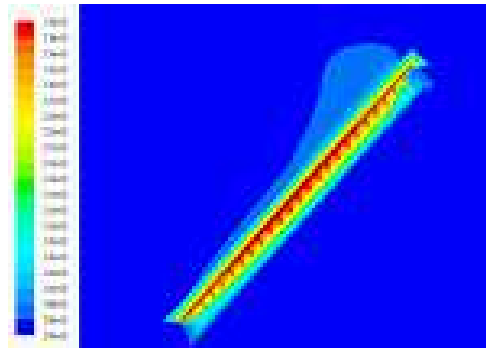


Fig. 13. temperature distribution diagram of solar panel with fins and 60mm air duct

the low. The temperature gradient at the top right of the solar panel is largest, and the temperature field distribution is irregular. At last, the heat mainly transfer to the top right of solar panels. The middle temperature of solar panel with fins and 60mm air duct is higher than the up and down. The temperature gradient at the top right of the solar panel is largest, But compared with the temperature gradient

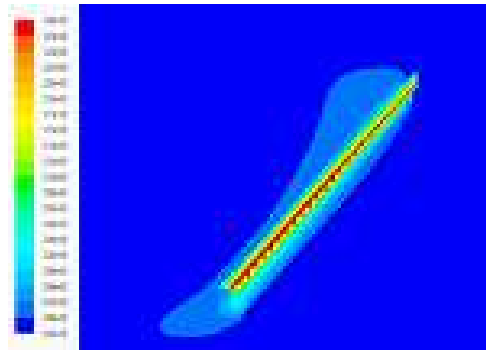


Fig. 14. temperature distribution diagram of solar panel with fins and 90mm air duct

at the top right of the solar panel which has fins and 30mm air duct, it is smaller. Also, the temperature field distribution is irregular, the heat mainly transfer to the top right of solar panels. The middle and low temperature of solar panel with fins and 90mm air duct is higher than the up. The temperature gradient at the top right and bottom of the solar panel is largest. Then the temperature field distribution is irregular, and the heat mainly transfer to the top right and bottom of solar panels.

It can be analyzed from the temperature distribution: the heat mainly transfer to the up of solar panels, then the top right, and last to the top right and bottom along with adding air duct and increase of distance about air duct, and the highest temperature part of the solar plate changes with the changing of heat.

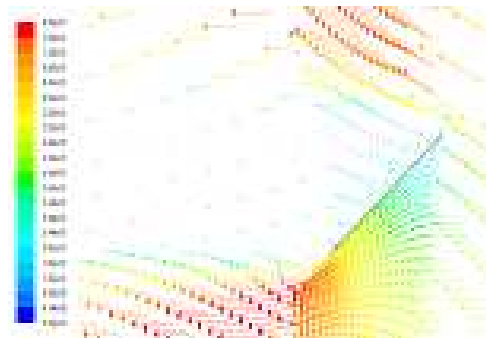


Fig. 15. velocity distribution diagram around the solar panel without fins

It can be seen through the velocity distribution diagram of solar panel: The low part wind velocity of solar panel is greater than the above wind velocity. And because of the high plate temperature and the low surrounding temperature, circulation is formed above the solar plate. Similarly, the high plate temperature and the low surrounding temperature formed air flow in the air duct of solar panel with fins and 30mm air duct, which flows from the bottom to the top. Small part air flow is formed at the top of the 60mm air duct, which points the lower. The left part air flow is formed the 60mm air duct, which points from bottom to top. And the

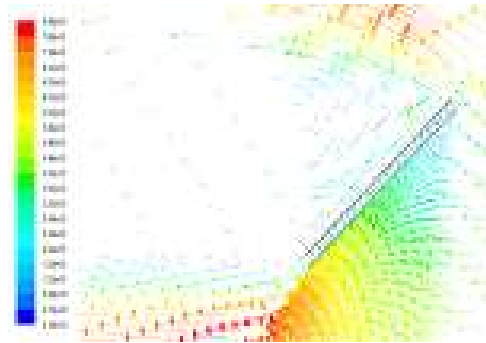


Fig. 16. velocity distribution diagram of solar panel with fins and 30mm air duct

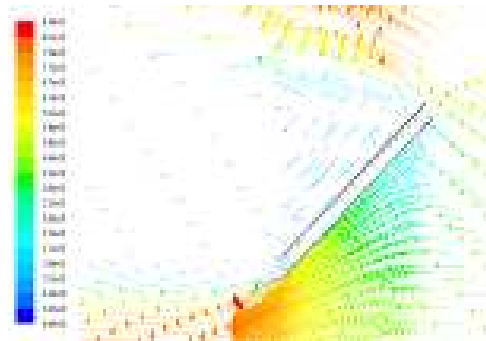


Fig. 17. velocity distribution diagram of solar panel with fins and 60mm air duct

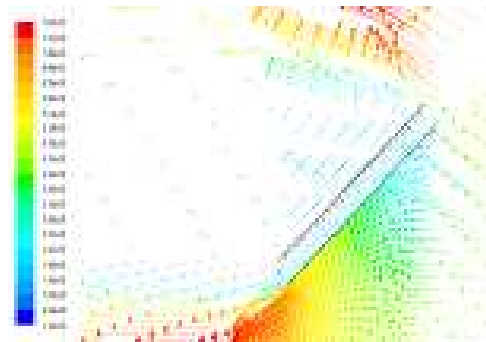


Fig. 18. velocity distribution diagram of solar panel with fins and 90mm air duct

velocity in 60mm air duct is less than the velocity in 30mm air duct. Micro air flow which points to the solar panels is formed between fins in the system of fins and 30mm air duct. And the left air flow which points from top to bottom is formed in the system of fins and 90mm air duct.

It can be analyzed from the velocity distribution: The wind velocity in the air duct presents female changing with the increase of air space, change from large to small, and become large again. The velocity changes from the bottom to the top,

then gradually changes from the top to the bottom.

From the line chart of the numerical simulation data produced by the FLUENT software, it can be observed that the solar panel surface temperature is changing when the solar panel has fins or without. The surface temperature distribution of solar panel is shown in figure 19 to figure 22.

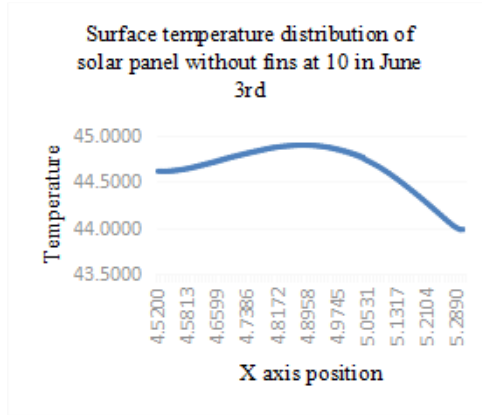


Fig. 19. surface temperature distribution of solar panels without fins

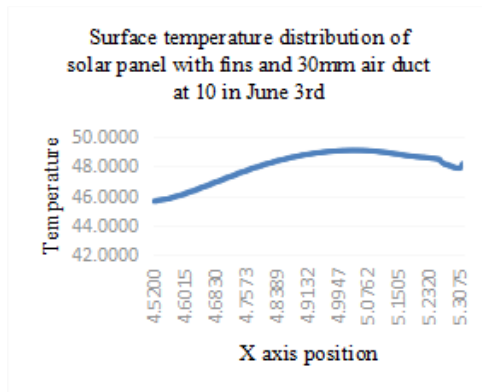


Fig. 20. surface temperature distribution of solar panels with fins and 30mm air duct

It can be seen through the temperature distribution diagram about photovoltaic solar panel of different circumstances at the same time: The temperature of solar panel which has air duct and fins is higher than the temperature of solar panel without fins. With adding air duct spacing, the solar panel temperature has changed. The temperature of low part is lower than the up part at first. Then the middle part temperature is higher than the both end part temperature. Finally the bottom part temperature is higher than the top part temperature. The change is consistent with the changes of temperature and velocity distribution diagram. It can be seen that the radiation effect of the solar panel which have fins and air duct is not better

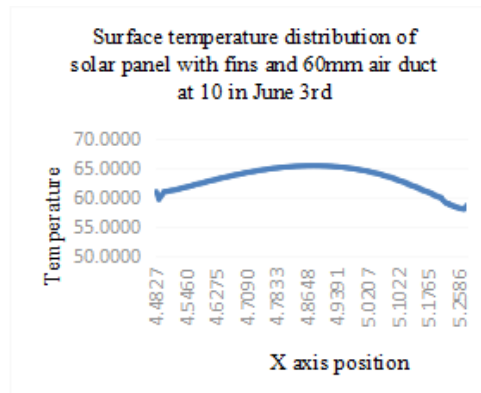


Fig. 21. solar panels with fins and 30mm air duct solar panels with fins and 60mm air duct

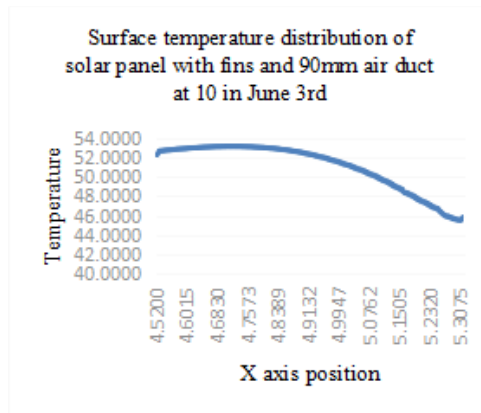


Fig. 22. surface temperature distribution of solar panels with fins and 90mm air duct

than the solar panel without fins.

#### 4. Conclusion

In this paper, the change of temperature distribution and heat dissipation about photovoltaic solar panel is analyzed. And the changes happen with different natural ventilation cooling modes and different outdoor conditions which include different outdoor temperature, wind speed and solar radiation. Consequently, a quantitative basis for the practical engineering has been provided in such aspects as design and construction. Moreover, a foundation has been laid for its popularization and application in the future.

## References

- [1] K. F. LI, J. L. REN: *Policy analysis of new energy industry development in China*. *Wireless interconnect technology* 11 (2013), 165.
- [2] AQEEL. AHMED. BAZMI, GHOLAMREZA. ZAHEDI: *Sustainable energy systems: role of optimization modeling techniques in power generation and supply—A review*. *Renewable and sustainable energy reviews* 15 (2011), 3480–3500.
- [3] ADNAN. IBRAHIM, MOHD. MYUSOF. OTHMAN, MOHD. HAFIDZ. RUSLA, SOHIF. MAT, KAMARUZZAMAN. SOPIAN: *Recent advances in flat plate photovoltaic/thermal (PV/T) solar collectors*. *Renewable and sustainable energy reviews* 15 (2011), 352-365.
- [4] J. J. CHEN: *China's experiment on the differential electricity pricing policy and the struggle for energy conservation*. *Energy policy* 39 (2011), No. 9, 5076-5085.
- [5] T. T. CHOW, L. S. CHAN, K. F. FONG, Z. LIN, W. HE, J. JI: *Annual performance of building-integrated photovoltaic/water-heating system for warm climate application*. *Applied energy* 86 (2009), 689-696.
- [6] Y. LI, A. DELSANTE: *Natural Ventilation Induced by Combined Wind and Thermal Forces*. *Building and environment* 36 (2001), 59-71.
- [7] CHARLES. D. CORBIN, ZHIQIANG. JOHN. ZHAI: *Experimental and numerical investigation on thermal and electrical performance of a building integrated photovoltaic thermal collector system*. *Energy and buildings* 42 (2010), 76-82.
- [8] SLAWOMIR. MIKULA, GILBERT. DE. MEY, ANDRZEJ. KOS: *Asynchronous control of modules activity in integrated systems for reducing peak temperatures*. *the VLSI journal* 41 (2008), 447-458.

Received November 16, 2016